Complex-salt model building using combination of interactive beam migration and localized RTM

Bin Wang, Chuck Mason, Kwangjin Yoon, Jean Ji, Jun Cai, TGS-NOPEC, Sang yong Suh, KIGAM

Summary

A new salt velocity model building methodology is proposed which allows effective testing of different salt interpretation scenarios. In this methodology, we combine the strength of efficiency from interactive beam migration with the accuracy of localized RTM to derive a more accurate salt geometry. Using interactive salt geometry editing and efficient beam migration, a large number of salt interpretation scenarios are quickly tested and narrowed down to a small number of likely salt interpretation cases. This is followed by a reduced number of localized RTM runs to single out the final salt velocity model. Redatuming the wavefield from surface to a user defined subsurface datum plays a pivotal role in this methodology; it enables improvement in the quality of beam migration and in the efficiency of RTM.

Introduction

Prestack depth migration has been used routinely for subsalt imaging in Gulf of Mexico (GOM). To produce a good subsalt image, an accurate velocity model is needed. The generation and refinement of the velocity model in a routine production project is often a complex process (Singer, 2005). The model typically has multiple embedded salt bodies of complex geometries

The need for accurate interpretation of salt and salt model building has been emphasized by many authors (Sayers and Herron, 2007; and Mosher et. al., 2007). The identification and definition of the shape of the salt geometry is a critical and time-consuming step for a successful subsalt imaging project. Salt interpretation can account for about 70% of a typical depth-imaging project as pointed out by Reasnor (2007).

The existing salt velocity model building methodology may not be effective in the complex areas where salt geometry is not clearly identifiable in the seismic migration image. The industry standard salt model building method follows a flow of sediment flood and salt flood. At every step of this standard flow only one top of salt (TOS) or one base of salt (BOS) interpretation is allowed. The fundamental assumption for this methodology is that salt boundary is well imaged by seismic migration, and therefore salt boundary is interpreted and picked with certainty. This may not true for areas with complex salt geometry, where salt geometry is not well defined by seismic migration images. In case of complex salt geometry, or for whatever reasons salt geometry is not well imaged, the standard salt model building methodology breaks down, and it demands a new more effective salt model building methodology.

Generally, salt model building and prestack depth migration is an iterative process that requires integration of salt interpretation and depth processing. Salt interpretation is often not clear-cut for a complex salt geometry, and often requires testing different interpretation scenarios, especially for base of salt (BOS) where imaging is often poor. Since a depth imaging project is an iterative process of velocity model building and depth migration, it is often desirable to develop fast depth migration algorithms for velocity model building (Hill, 1990; Wang and Pann, 1996; Sun, Y. et. al., 2000; Hua and McMechan, 2001, 2003; Sun and Schuster, 2003; Fei and McMechan, 2006, Liu and Palacharla, 2008; Wang et al., 2008).

Although still expensive, Reverse Time Migration (RTM) has shown great potential not only as a final imaging tool, but also as a velocity model building tool. RTM has high accuracy in modeling complex wave propagation including turning waves and multiply bounced waves such as prism waves (Jones, 2007). RTM not only defines steep-dip boundaries better, it also shows great potential to image shadow zones improving event termination towards salt boundary and better imaging rugose TOS and BOS. Therefore, RTM shows great potential to define a more accurate salt model, especially for complex salt geometry (Yoon et. al. 2008; Ortigosa et. al., 2008; Liu and Wang, 2008)

New methodology of salt model building

The basic assumption of the current standard methodology of salt model building is that TOS is clearly defined by sediment flood migration image, and BOS is well defined by salt flood migration image. In many complex areas, salt boundary is not clearly identifiable by seismic imaging, especially when there are multiple salt bodies in close proximity. In case of a deeper second salt body, it is seldom we can interpret the second deeper salt geometry with any certainty. Many interpretation scenarios need to be tested out before finalizing the salt interpretation. Clearly the existing standard salt model building methodology is not effective for building such complex salt models.

The proposed methodology takes advantage of the sensitivity of seismic depth migration on salt geometry. In some areas such as GOM, due to high velocity contrast between low velocity sediment and high velocity salt, accuracy of the salt geometry has the first order impact on depth migration image quality in the areas around or beneath salt bodies.

There are two key components in the proposed salt model building methodology: 1) Interactive beam migration; 2) Localized RTM. The efficient interactive beam migration tools (Wang et. al., 2008) are used to quickly test very broad range of salt interpretation scenarios. Typically about 20 to 30 salt models are tested by using interactive beam migration, and are narrowed down a smaller number of more possible salt interpretation scenarios (for example 3 to 5 models). Then more accurate and high quality localized RTM (Yoon et. al., 2008) are used to nail down one final model from the remaining 3 to 5 models.

Interactive beam migration for salt model building

The inputs for our interactive beam migration flow are prestack depth migration volume and its associated velocity model. Figure 1 shows the flow chart of how we perform salt interpretation scenario testing, using the interactive beam migration tools.

We first perform a wave-equation based post-stack demigration to a subsurface datum, above which the velocity model is finalized. Typically the subsurface datum is directly below the TOS. By doing the down going migration (done when we get the PSDM volume), and up going demigration, we effectively achieved a wavefield redatuming from surface to this subsurface datum.

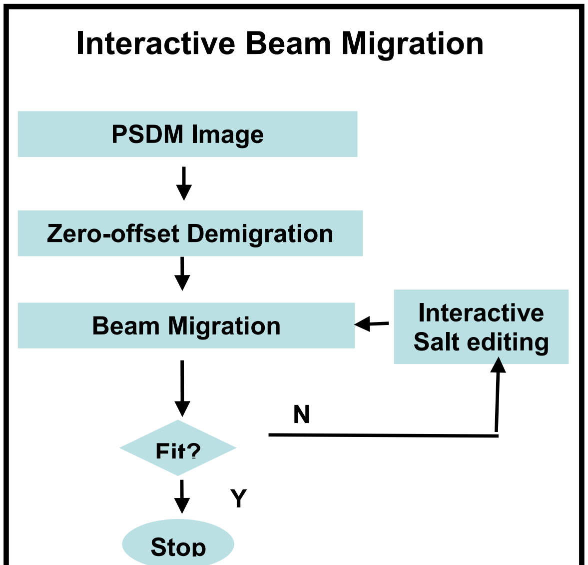

Figure 1: Flow chart of interactive beam migration for testing different salt interpretation scenarios.

The demigrated wavefield is used as the input for beam migration to test different salt interpretation scenarios. One of the efficient components in the interactive beam migration flow is the polygon-based interactive salt editing tool, which enables us to quickly and interactively add or remove a segment of salt (Wang et. al., 2008).

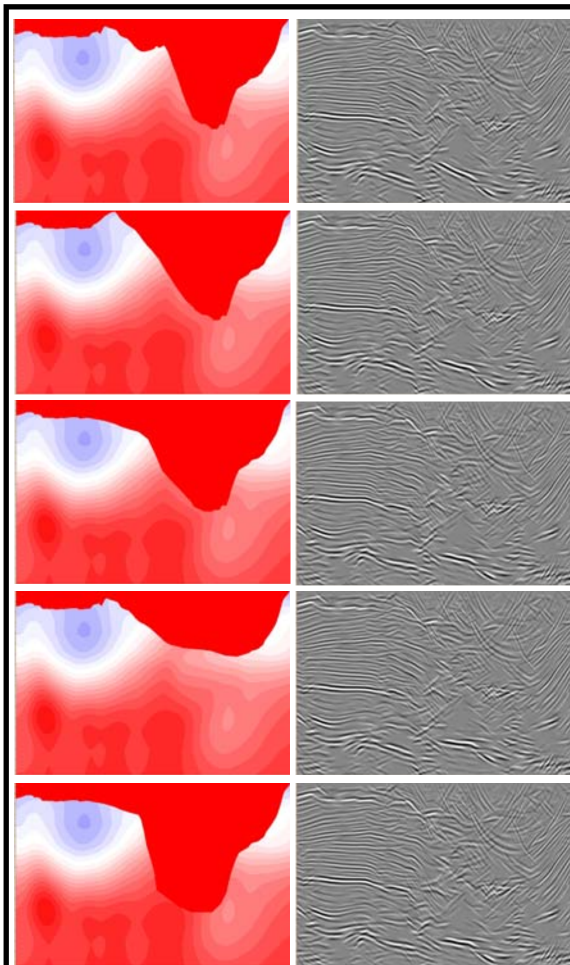

***Figure 2**: Left column shows different salt interpretations and velocity models; Right column shows the corresponding beam migration images using the velocity models on its left.*

Figure 2 shows a few examples of salt velocity models and the corresponding beam migration images for a 3D data set from GOM. It is not clear on seismic image whether or not there is a salt6 keel and how deep the salt keel might be. For this example, more than 20 salt models are tested using the interactive beam migration tools, and narrowed down to three models which are further tested by using more accurate local RTM.

Localized RTM for salt model building

To make RTM more affordable to test several possible salt interpretations, such as how deep the salt keels go (Figure 3), we first perform RTM-based wavefield redatuming, which redatums the shot-based wavefield from the surface to a subsurface datum above which the salt geometry is fixed.

There are a few important benefits of performing RTM-based wavefield redatuming. The computation cost can be dramatically reduced by only performing RTM using the redatumed wavefield below the subsurface datum due to the following two main factors. First, the computation grid size can be greatly increased while still being able to avoid dispersion noise, because the minimum velocity is much higher at greater depth. For example, assuming the minimum velocity is increased from 1.5 km/s at surface to 2.5 km/s at redatuming surface of 6 km depth (assuming velocity increases with depth), the computation grid size can be increased by a factor of 1.67, considering 3 dimensions in space and one dimension in time which would translates to speed-up by a factor of 7. Second, the migration aperture can be much reduced. The required migration aperture is linearly proportional to the target depth. The computation savings due to the smaller required aperture is true for both the RTM-redatuming step as well as the subsequent multiple RTM runs using the redatumed wavefield. Additional cost saving can be achieved by identifying and pre-selecting only those input shots which contribute/illuminate the target areas. Other benefits of using redatuming for RTM, such as saving on computer memory et. al., are discussed in Guan et. al., (2008).

Figure 4 shows the flow chart for our localized RTM. First, input shot gathers (or selected shot gathers) are redatumed from the surface to a user-defined subsurface datum. On the source side, the forward-modeled wavefields are saved to local disk for the redatuming surface at a given time interval. One alternative view of source-side redatuming is that it converts a point source at the surface into area sources in the subsurface datum. On the receiver side, the receiver wavefields (input shot records) are reverse-time propagated and wavefields on the redatuming surface are saved to local disk. The saved redatumed wavefield is used to test different salt velocity models by performing multiple RTM runs.

We have developed a 3D RTM-based redatuming tool to redatum the wavefield from the surface to a subsurface datum. Figure 5 shows an example of the effectiveness of the 3D RTM-based redatuming. Figure 5A is a 3D RTM image generated by performing an one-step RTM run using the surface input data; Figure 5B is the corresponding RTM image from using the redatumed wavefield at 6 km depth. Except some visible amplitude difference, the two image qualities are very comparable.

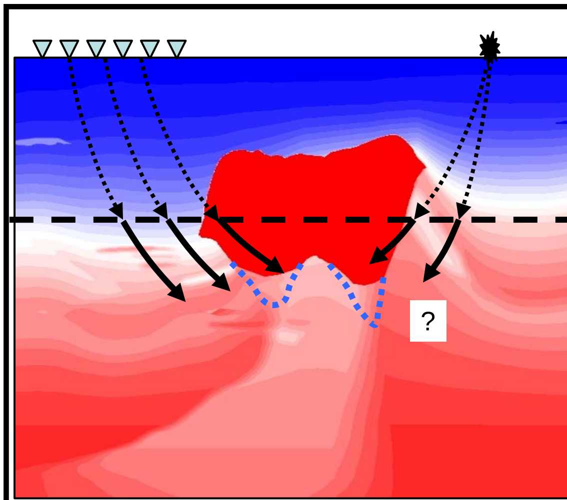

Figure 3*: Schematic diagram showing redatuming of both receiver side and source side wavefields from surface to a subsurface datum.*

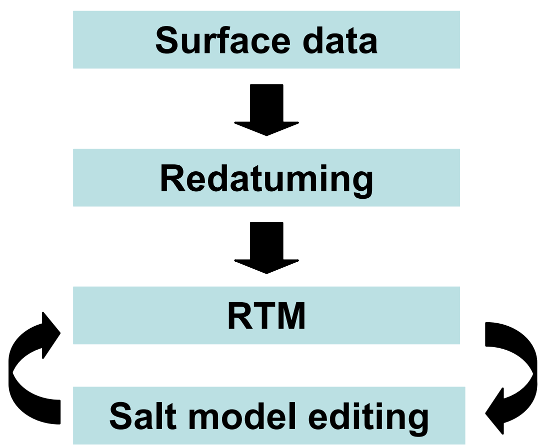

Figure 4*: A) RTM image using surface input data; B) RTM image using redatumed wavefield.*

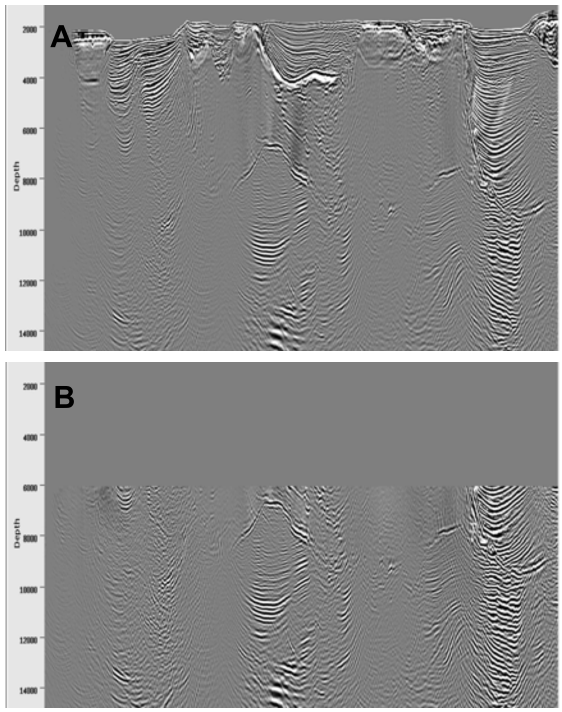

***Figure 5**: A) RTM image using surface input data; B) RTM image using redatumed wavefield.*

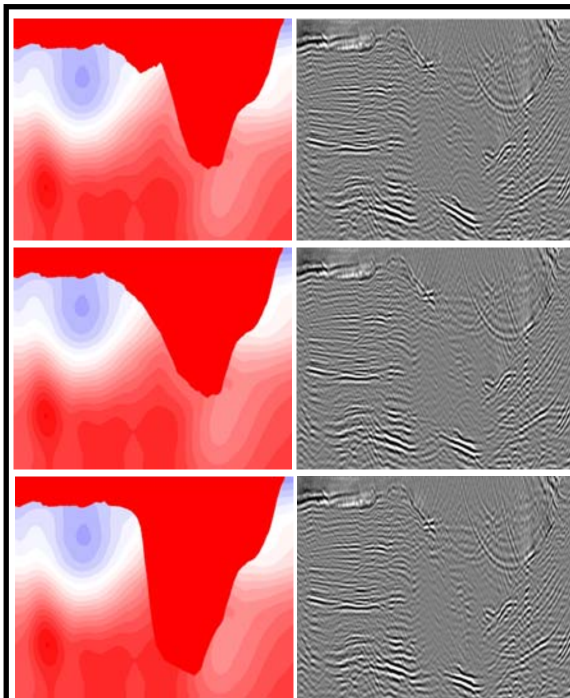

***Figure 6**: Left column shows different salt interpretations and velocity models; Right column shows the corresponding localized RTM images using the velocity models on its left.*

One technical challenge we have to face and resolve is the "data explosion" problem. A typical 3D NAZ survey only has 6 to 8 cables, and even a development WAZ survey has only up to 80 cables in a super shot gather. However, after redatuming, in the xline direction we need to save a few hundred lines. So the data volume could be exploded by one to two orders of magnitude. To solve the "data explosion" problem, we have developed a wavelet-transform based data compression technique which is able to achieve a compression ratio of 10:1 to 50:1.

Figure 6 shows an example of how localized RTM is used to test different salt velocity models. This is the same 3D data set shown in Figure 2. Interactive beam migrations are used to test more than 20 different salt geometries, and three more likely salt models (Figure 6, left column) are narrowed down, then localized RTM is used to produce the RTM images shown in right column of Figure 6. Based on the RTM image, the bottom salt geometry is chosen to be the final model, which makes more geological sense.

Conclusions

We have developed an effective salt model building methodology which allows effective testing of many different salt interpretation scenarios. The new methodology takes advantage of the sensitivity of a migration image to salt geometry changes. The efficient beam migration and practical interactive salt editing tools allow us to quickly test a large number of salt interpretation scenarios. The accuracy of RTM, especially in areas around and beneath the salt bodies, makes it an effective tool to build a good salt model.

Wavefield redatuming plays an important role in this methodology. Redatuming the wavefield enables a layer-stripping type of salt model building approach. For the interactive beam migration step, the redatuming is achieved by wave-equation based down-going migration and up going demigration; and for the localized RTM step, the redatuming is directly achieved in the shot domain. Data compression is a practical way to address the "data explosion" problem of 3D redatuming.

Acknowledgments

We would like to thank Zhiming Li, Young Kim, Eric Nessler, and Wilfred Whiteside for their interests and helpful discussions. We thank TGS-NOPEC management for permission to publish this paper.

EDITED REFERENCES

Note: This reference list is a copy-edited version of the reference list submitted by the author. Reference lists for the 2009 SEG Technical Program Expanded Abstracts have been copy edited so that references provided with the online metadata for each paper will achieve a high degree of linking to cited sources that appear on the Web.

REFERENCES

Fei, W., and G. McMechan, 2006, 3D common-reflection-point-based seismic migration velocity analysis: Geophysics, **71**, no. 5, S161–S167.

Guan, H., Z. Li, B. Wang, and Y. Kim, 2008, A multi-step approach for efficient reverse-time migration: 78th Annual International Meeting, SEG, Expanded Abstracts, 2341–2345.

Hill, N. R., 1990, Gaussian Beam migration: Geophysics, **55**, 1416–1428.

Hua, B. L., and G. A. McMechan, 2001, Parsimonious 2-D post-stack Kirchhoff depth migration: Geophysics, **66**, 1497–1503.

Jones, I., M. C. Goodwin, I. D. Berranger, H. Zhou, P. A. Farme, 2007, Application of anisotropic 3D reverse time migration to complex North Sea imaging: 77th Annual International Meeting, SEG, Expanded Abstracts, 2140–2143.

Liu, J., and G. Palacharla, 2008, Multi-arrival Kirchhoff beam migration: 78th Annual International Meeting, SEG, Expanded Abstracts, 2311–2315.

Liu, W, and Y. Wang, 2008, Target-oriented reverse time migration for two-way prestack depth imaging: 78th Annual International Meeting, SEG, Expanded Abstracts, 2326–2330.

Mosher, C., E. Keskula, J. Malloy, R. Keys, H. Zhang, and S. Jin, 2007, Iterative imaging for subsalt interpretation and model building: The Leading Edge, **26**, 1424–1428.

Ortigosa, F., Q. Liao, A. Guitton, and W. Cai, 2008, Speeding up RTM velocity model building beyond algorithmics: 78th Annual International Meeting, SEG, Expanded Abstracts, 3219–3223.

Reasnor, M. D., 2007, Salt interpretation practices for depth imaging in the Gulf of Mexico: The Leading Edge, **26**, 1438–1441.

Singer, P., 2005, Subsalt imaging: Is the salt winning?: SEG/EAGE Summer Workshop.

Sayers, C., and D. Herron, 2007, Introduction to this special section: Subsalt exploration: The Leading Edge, **26**, 1404–1405.

Sun, H., and J. Schuster, 2003, 2D wavepath migration: Geophysics, **66**, 1528–1537.

Sun, Y. H, F. H. Qin, S. Checkles, and J. P. Leveille, 2000, 3-D prestack Kirchhoff beam migration for depth imaging: Geophysics, **65**, 1592–1603.

Wang, B., and K. Pann, 1996, Kirchhoff migration of seismic data compressed by matching pursuit decomposition: 66th Annual International Meeting, SEG, Expanded Abstracts, 1642–1645.

Wang, B., J. Jean, C. Mason, S. Gajawada, and Y. Kim, Beam-based interactive imaging for salt interpretation and salt model building: 78th Annual International Meeting, SEG, Expanded Abstracts, 3073–3077.

Wang, B., Y. Kim, C. Mason, and X. Zeng, 2008, Advances in velocity model-building technology for subsalt imaging: Geophysics, **73**, no. 5, VE173–VE181.

Yoon, K., B. Wang, Y. Kim, and H. Guan, 2008, Localized reverse time migration for salt model building: 78th Annual International Meeting, SEG, Expanded Abstracts, 2331–2335.